31st Annual International Conference of the IEEE EMBS
Minneapolis, Minnesota, USA, September 2-6, 2009

Tissue Characterization Using Multiscale Products of Wavelet Transform of Ultrasound Radio Frequency Echoes

Mohammad Aboofazeli, Purang Abolmaesumi, Gabor Fichtinger, and Parvin Mousavi

Abstract— **This paper presents a novel method for tissue characterization using wavelet transform of ultrasound radio frequency (RF) echo signals. We propose the use of multiscale products of wavelet transform sequences of RF echoes to estimate the scatterer distribution in the tissue. The proposed method is based on the fact that when emitted ultrasound beams interact with scatterers in the tissue, backscattered beams contain singularities corresponding to the location of the scatterers. The singularities will exist in multiple scales of wavelet sequences of the echo signals. Therefore, peaks of wavelet transform multiscale products correspond to the location of scatterers. Estimation of scatterer spacing can be used for tissue characterization. The efficacy of the proposed method was validated in RF echo signals of *in-vitro* human prostate to characterize normal and cancerous tissue. The results confirm that wavelet transform multiscale products of RF echo signals contain tissue typing information that can be used as an effective tool to differentiate normal and cancerous prostate tissue.**

I. Introduction

ULTRASOUND imaging is the modality of choice for a wide variety of medical diagnostic procedures. Safety, cost effectiveness, portability, and real-time nature of ultrasound imaging are among advantages of this modality; however, poor visibility of many abnormalities in ultrasound images is a drawback for this imaging modality.

For example, prostate biopsy is a diagnostic procedure in which transrectal ultrasound (TRUS) imaging is used for identifying the outline of the prostate and guiding the biopsy needle to predefined anatomical regions of the prostate. Conventional biopsy under TRUS guidance has poor sensitivity, with positive predictive values between 40 and 60% [1]. More accurate biopsy targeting and cancer diagnosis could be achieved if samples were taken not only from predefined locations of the prostate, but also from specific locations where the image can predict cancer with reasonably high probability; However, B-mode ultrasound images do not have image-specific targeting capability.

Numerous techniques have been proposed for computer-aided detection of prostate cancer using ultrasound images to facilitate image-specific targeting [2]. Many techniques are based on texture features of ultrasound B-scan images [3]-[5]; However, as shown in [6]-[8], some of the tissue characterizing parameters can only be extracted from RF echo signals before they are processed for B-mode image generation.

RF echo signals have been successfully used to characterize tissue types with applications in cancer diagnosis. Tissue characterizing parameters extracted from RF signals include those describing the attenuation and scattering of ultrasound in the tissue. Feleppa *et al*. [7] have used the normalized power spectra of RF echo signals for prostate tissue typing. They derive the intercept, slope and mid-band values of the linear regression of the frequency spectrum of RF signals for tissue typing.

Estimation of scatterer spacing is another technique proposed for tissue characterization using RF echo signals. Scatterer spacing has previously been performed using two different approaches in the literature: Spectral analysis and wavelet analysis. Spectral analysis methods include techniques based on estimation of the autocorrelation function [9], cepstrum [10], spectral autocorrelation [11, 12], generalized spectrum [13], complex cepstrum [14] and singular spectrum analysis (SSA) [15]. Spectral techniques work on the assumption that the analyzed signal is stationary; this is not the case for most RF echo signals [16]. Wavelet transform based techniques include the use of modulus maxima [17] and continuous wavelet transform [18] for tissue characterization.

In this study, detection of peaks of wavelet transform multiscale products (WTMSP) of ultrasound RF echoes is proposed as a novel wavelet-based method for estimation of scatterer spacing. Accuracy of the proposed method is investigated in simulated RF echoes. Furthermore, the efficacy of WTMSP peak detection in quantitative analysis of echo patterns as a feature for tissue typing in *in-vitro* human prostate is studied. The results of tissue classification using proposed method are compared to those of the method suggested in [7] which has been a pioneering work in the prostate tissue typing based on RF echo signals.

Manuscript received April 7, 2009. This work was supported in part by Natural Sciences and Engineering Research Council of Canada (NSERC) and the Canadian Urological Association.

M. Aboofazeli is with the Queen's University, Kingston, ON K7L 3N6, Canada (phone: 613-533-2797; e-mail: mohammad@ cs.queensu.ca).

P. Abolmaesumi is with the School of Computing, Department of Electrical and Computer Engineering, and Department of Surgery, Queen's University, Kingston, ON K7L 3N6, Canada. (e-mail: purang@cs.queensu.ca).

G. Fichtinger is with the School of Computing, Department of Electrical and Computer Engineering, and Department of Mechanical and Materials Engineering, Queen's University, Kingston, ON K7L 3N6, Canada. (e-mail: gabor@cs.queensu.ca).

P. Mousavi is with the School of Computing, Queen's University, Kingston, ON K7L 3N6, Canada. (e-mail: pmousavi@cs.queensu.ca).

II. METHODS

A. Ultrasound RF echo signal modeling

The RF echo signals are formed by three-dimensional convolution of tissue structures and ultrasound pressure waves. Analysis of RF echo signals in three-dimensional space is a challenging task. In this study, the point scatterer model is used which is a simplified model based on the assumptions of narrow ultrasound beam, weak scattering and linear propagation [19]. In this model, RF echo signal $y(t)$ is modeled by:

$$y(t) = h(t) * s(t) + \omega(t), \tag{1}$$

where $h(t)$ and $s(t)$ are the transmitted ultrasound pulse wave and the scatterer distribution, respectively and $\omega(t)$ is additive white noise. Scatterer distribution $s(t)$ can be decomposed into two components:

$$s(t) = \sum_{n=1}^{N_R} r_n(t - \varphi_n) + \sum_{n=1}^{N_D} d_n(t - \theta_n), \tag{2}$$

where N_R and N_D are, respectively, the number of resolvable and diffused scatterers, $r_n(.)$ and $d_n(.)$ are scatters generated by *n-th* resolvable and diffused scatterers, and φ_n and θ_n are time delays corresponding to the distance of scatterers to the transducer. If we define

$$R(t) = \sum_{n=1}^{N_R} r_n(t - \varphi_n) * h(t) \tag{3}$$

and

$$D(t) = \sum_{n=1}^{N_D} d_n(t - \theta_n) * h(t), \tag{4}$$

then $y(t)$ is given by

$$y(t) = R(t) + D(t) + \omega(t), \tag{5}$$

where $R(t)$ and $D(t)$ are the terms corresponding to resolvable and diffused scatterers, respectively.

B. Multiscale product of wavelet transform

Wavelet transform decomposes a signal into band limited components, which can be reassembled to reconstruct the original signal without error [20]. Wavelet transform is linear; therefore, wavelet transform of RF echo signal at scale 2^j, $W_j[.]$ is denoted as:

$$W_j[y(t)] = W_j[R(t)] + W_j[D(t)] + W_j[\omega(t)], \tag{6}$$

As shown in [17], resolvable scatterers will lead to singularities in the echo signal at the times corresponding to their locations in space. These singularities in the echo signals will lead to local maxima in $W_j[R(t)]$ at all scales. On the other hand, diffused scatterers will lead to local maxima in the wavelet transform at middle scales. These local maxima will disappear at lower scales as well as at very high scales. White noise will lead to local maxima at lower scales only. Therefore, local maxima of wavelet transform at high scales are generated by resolvable scatterers [17]. Based on these facts, it has been suggested that multiplying the wavelet transform coefficients at adjacent high scales will amplify the maxima corresponding to singularities generated by resolvable scatterers, whereas it reduces the maxima corresponding to diffused scatterers and noise [21], [22].

In this study, wavelet transform sequences of RF echo signals are decomposed to five levels (scale $2^5 = 16$). The products of wavelet sequences at scales $2^4 = 16$ and $2^5 = 32$ are calculated and their local maxima are located and average distance between the local maxima is estimated as mean scatterer spacing.

C. Simulation Data

In order to validate the distances between resolvable scatterers estimated by the proposed method, RF echo signals were firstly simulated using Field II ultrasound simulation program [23] with a number of resolvable scattering particles with equal distance. Estimated scatterer spacing was then compared to the particle distance set in the simulation. All physical dimensions of the simulation probe were set to those of real transrectal probe used in *in-vitro* prostate imaging. Center frequency of the simulation probe was set to 6.6 MHz.

D. Experimental Data

The experimental data was collected from extracted prostate specimens of 35 patients who chose prostatectomy as their treatment option [24]. Extracted prostates were scanned along parallel planes that were 4 mm apart while the prostates were suspended in a water bath. RF echo signals were recorded using a Sonix RP (Ultrasonix Inc., Richmond, BC, Canada) ultrasound machine equipped with a transrectal probe (BPSL9-5/55/10).

The prostate specimens were then dissected along the scanned cross-sections at 4 mm intervals. Histopathological malignancy maps of whole mount slides were acquired and used as the gold standard. In order to evaluate the results of ultrasound-based techniques for prostate cancer detection,

the results were compared with the maps acquired by the histopathological analysis of the same cross section of tissue. The process of registering the histopathology maps to the RF frames was performed manually using visual landmarks.

Due to the elevation beam width of ultrasound signals and also inevitable errors caused by the low precision cutting process in the pathology lab, the accurate match between tumor boundaries in ultrasound and histopathology images was challenging. Therefore, only a limited number of ROIs from cross-sections for which a high level of confidence of registration could be achieved were selected. In each cross-section, several regions of interest (ROIs) with size of 96 × 8 pixels (3.7 × 1.87 mm) were chosen. ROIs were selected from 46 cross-sections. 1478 normal and 856 cancerous ROIs were selected for this study.

WTMSP of echo signals in each ROI were computed. Distances between local maxima of WTMSP were then averaged and used as a representative feature of ROI for quantitative analysis of the RF echo signals.

III. Results and Discussion

A. Simulation Results

RF echo signals were simulated using Field II simulation program. As ultrasound center frequency was set to 6.6 MHZ, wavelength of the ultrasound beam was 233 micrometers. Distances between resolvable scattering particles were estimated when scatterer spacing in simulation were set to equal distances of 250-400 micrometers. Figure 1 shows an example of simulated RF echo signal (contaminated with Gaussian additive noise at SNR=10 dB) when the distance between particles was set to 270 microns. Estimated average distance between detected locations of scatterers is 263 microns which is very close to the scattering particles (less than 3% error). Estimation error for particles with distances in the range of 250-400 micrometers was less than 4%. Therefore, the proposed algorithm is able to successfully estimate distances between resolvable scatterers in the presence of additive noise.

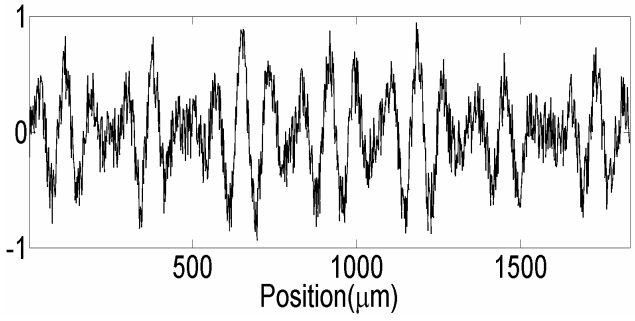

Figure 1: An example of simulated RF echo signals where scatterer spacing is 270 micrometers.

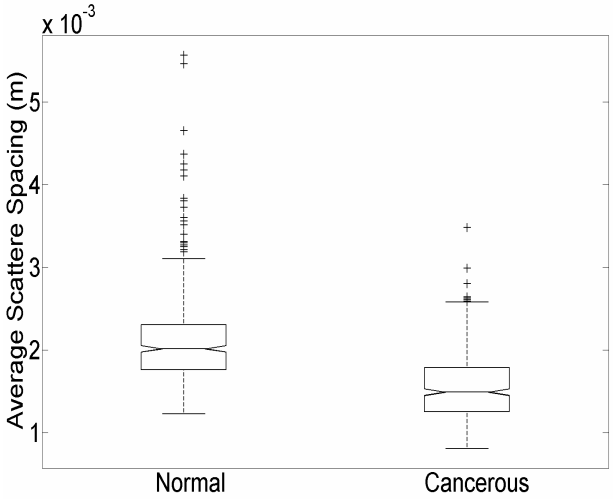

Figure 2: Average scatterer spacing in normal and cancerous prostate tissue.

B. Experimental Results

Distances between local maxima of WTMSP of RF echo signals collected from normal and cancerous prostate tissue were estimated. We tested the samples of the local maxima distances from normal and cancerous prostate tissues using ANalysis Of VAriance (ANOVA) test with the null hypothesis of the equality of means in samples from two different populations. This test resulted in *p*-value of almost zero which rejects the null hypothesis. This can be interpreted as significant difference between distances between local maxima of WTMSP in normal and cancerous prostate.

Figure 2 displays the distribution of the distance in normal and cancerous samples around their medians using a box and whisker plot. The line in the middle of each box is the sample median, the tops and bottoms of each box are the 25th and 75th percentiles of the samples, respectively, and the distances between the tops and bottoms are the inter-quartile ranges. The whiskers (lines extending above and below each box) are drawn from the ends of the inter-quartile ranges to the furthest observations within the whisker length. Observations beyond the whisker length are marked as outliers (displayed with + sign). It can be seen that only the top 25 percent of cancerous tissue and bottom 25 percent of normal tissue overlap. Therefore, this figure is evidence confirming significant difference between distances between local maxima of WTMSP in normal and cancerous prostate tissue.

A support vector machine (SVM) classifier was used to classify the ROIs using WTMSP features. Classification accuracy, sensitivity and specificity of this classifier along with those of SVM classifier using spectral features introduced in [7] are shown in Table I. As it can be seen the accuracy of the classifier using WTMSP is almost the same as that of spectral feature-based classifier. However,

TABLE I
COMPARISON OF CLASSIFICATION PERFORMANCE OF THE PROPOSED TISSUE TYPING APPROACH WITH THE FELEPPA SPECTRAL FEATURES

	WTMSP	Spectral Features [a]
Accuracy	73%	72.3%
Sensitivity	76.4%	52.8%
Specificity	70%	82.1%

[a] As calculated and reported in [25].

WTSMP based classifier has a better sensitivity. As false negative diagnosis is a major problem in the conventional biopsy procedure, increasing sensitivity is a very important advantage for the classifier based on WTMSP.

IV. CONCLUSION

This study proposes a novel wavelet-based method for estimation of scatterer spacing. The method is based on detection of peaks of wavelet transform multiscale products of ultrasound RF echoes. In order to validate the mean scatterer spacing estimated by the proposed method, echo signals were simulated using Field II simulation program when scatterer spacing in simulation were set to equal distances of 250-400 micrometers. The proposed algorithm was able to estimate distances between resolvable scatterers with less than 4% error. The accuracy of the proposed algorithm can be further studied with a real probe in a tissue mimicking phantom with known scatterer distribution. This is the subject of our future work.

Also, through *in-vitro* human prostate data, it was shown that estimation of average distance of WTMSP local maxima may function as a feature for tissue typing. ANOVA test confirmed that the local maxima distances from normal and cancerous prostate tissues are significantly different. An SVM classified the normal and cancerous ROIs using WTMSP features with sensitivity better than an SVM classifier that used spectral features proposed in [7].

REFERENCES

[1] T. Goossen, J. de la Rosette, C.A. Hulsbergen, G. van Leenders ,and H. Wijkstra, "The value of dynamic contrast enhanced power Doppler ultrasound imaging in the localization of prostate cancer," *European Urology*, vol. 43, no. 2, pp. 124 –131, February 2003.

[2] M. Moradi, P. Mousavi, and P. Abolmaesumi, "Computer-aided diagnosis of prostate cancer with emphasis on ultrasound-based approaches: A review," *Ultrasound Med Biol*, vol. 33, no. 7, pp. 1010-1028, 2007.

[3] U. Scheipers, A. Lorenz, A. Pesavento, H. Ermert, H.J. Sommerfeld, M.Garcia-Schurmann, K. Kuhne, T. Senge, and S. Philippou, "Ultrasonic multifeature tissue characterization for prostate diagnosis," *Ultrasound Med Biol*, vol. 29, no. 8, pp. 1137–1149, 2003.

[4] O. Basset, Z. Sun, J.L. Mestas, and G. Gimenez, "Texture analysis of ultrasonic images of the prostate by means of co-occurrence matrices," *Ultrasonic Imaging,* vol. 15, no. 3, pp. 218 –237, 1993.

[5] M.J.F. Valckx, and M.J. Thijssen, "Characterization of echocardigraphic image texture by co-occurrence matrix parameters," *Ultrasound Med Biol*, vol. 23, no. 4, pp. 559 –571, 1997.

[6] A.J. Jensen, "Imaging of complex media with acoustic and seismic waves," In *topics in applied physics. Ultrasound and its modeling,* vol.84, pp. 135–164, Springer-Verlag, Berlin, Germany, 2002.

[7] E.J. Feleppa, A. Kalisz, J.B. Sokil-Melgar, F.L. Lizzi, T. Liu, A.L. Rosado, M.C. Shao, W.R. Fair, Y. Wang, M.S. Cookson, V.E. Reuter, and W.D.W. Heston, "Typing of prostate tissue by ultrasonic spectrum analysis," *IEEE Trans. Ultrason. Ferroelect. Freq. Cont.*, vol. 43, no. 4, pp. 609–619, 1996.

[8] Lizzi, F.L., Feleppa E.J., Alam, S.K., and Deng, X.C., "Ultrasonic spectrum analysis for tissue evaluation," *Pattern Recognition Letters,* vol. 24, pp. 637– 658, 2003.

[9] L. L. Fellingham and P. G. Sommer, "Ultrasonic characterization of tissue structure in the in vivo human liver and spleen,'' *IEEE Trans. Son. Ultrason.*, vol. 31, pp. 418-428, July 1984.

[10] L. Landini and L. Verrazzani, "Spectral characterization of tissue microstructure by ultrasound: A stochastic approach," *IEEE Trans. Ultrason. Ferroelect. Freq. Cont.*, vol. 37, pp. 448-456, Sept. 1990.

[11] K. D. Donohue, J. M. Bressler, T. Varghese, and N. M. Bilgutay, "Spectral correlation in ultrasonic pulse-echo signal processing," *IEEE Trans. Ultrason. Ferroelect. Freq. Cont.*, vol. 40, pp. 330-337, July 1993.

[12] T. Varghese and K.D. Donohue, "Mean scatterer spacing estimateswith spectral correlation," J. Acoust. Soc. Amer., vol. 96, no. 6, pp. 3504-3515, Dec. 1994.

[13] Donohue KD, Huang L, Burks T, Forsberg F, Piccoli CW. Tissueclassification with generalized spectrum parameters. *Ultrasound Med Biol*, vol. 27, no. 11, pp. 1505–1514, 2001.

[14] R. S. Mia, M. H. Loew, K.A. Wear and R.F. Wagner, "Quantitative Estimation of Scatterer Spacing from Backscattered Ultrasound Signals Using the Complex Cepstrum," Lecture Notes in Computer Science , vol. 1230, pp. 513-518, 1997

[15] Pereira WCA, Bridal SL, Coron A, and Laugier P., "Singular spectrum analysis applied to backscattered ultrasound signals from in vitro human cancellous bone specimens," *IEEE Trans. Ultrason. Ferroelect. Freq. Cont.*, vol. 51, no. 3, pp. 302–312, 2004.

[16] X. Tang, U.R. Abeyratne, "Wavelet transforms in estimating scatterer spacing from ultrasound echoes," *Ultrasonics*, vol. 38 (1–8), Elsevier Science B.V., The Netherlands, pp. 688–692, 2000.

[17] U. R. Abeyratne, X. Tang, "Ultrasound scatter-spacing based diagnosis of focal diseases of the liver," *Biomed Sig Proc Cont*, vol. 2, pp. 9–15, 2007.

[18] Georgia Georgiou and Fernand S. Cohen, "Tissue Characterization Using the Continuous Wavelet Transform Part I: Decomposition Method," *IEEE Trans. Ultrason. Ferroelect. Freq. Cont.*, vol. 48, no. 2, March 2001.

[19] K. A. Wear, R. F. Wagner, M. F. Insana, and T. J. Hall, "Application of autoregressive spectral analysis to cepstral estimation of mean scatterer spacing," *IEEE Trans. Ultrason., Ferroelect., Freq. Contr.*, vol. 40, pp. 50-58, Jan. 1993.

[20] S. G. Mallat, *A Wavelet Tour of Signal Processing*. San Diego, CA, Academic Press, 1998.

[21] Y. Xu, J. B. Weaver, D. M. Hearly Jr, and J. Lu, "Wavelet transform domain filters: A spatially selective noise filtration technique," *IEEE Trans. Image Processing*, vol. 3, no. 6, pp. 747-758, 1994.

[22] B. M. Stadler and A. Swami, "Analysis of multiscale products for step detection and estimation," *IEEE Trans. Information Theory*, vol. 45, no. 3, pp. 1043-1051, 1999.

[23] J. A. Jensen, "Field: A program for simulating ultrasound systems," Medical & Biological Engineering & Computing, vol. 34, Supplement 1, Part 1, pp. 351-353, 1996.

[24] M. Aboofazeli, P. Abolmaesumi, M. Moradi, E. Sauerbrei, R. Siemens, A. Boag, and P. Mousavi, "Automated detection of prostate cancer using wavelet transform features of ultrasound RF time series," in *Medical Imaging : Computer-Aided Diagnosis*, ed. by N. Karssemeijer, M.L. Giger, Proc. of SPIE, Vol. 7260, pp. 72603J1-8, 2009

[25] M. Moradi, P. Mousavi, R. Siemens, E. Sauerbrei, A. Boag, and P. Abolmaesumi, "Prostate cancer probability maps based on ultrasound RF time series and SVM classifiers: A large scale in-vitro study" In: D. Metaxas et al. (eds.) *Lecture Notes in Computer Science*, vol. 5241, pp. 76–84, 2008.